

A nonlinear PI and backstepping based controller for tractor-steerable trailer influenced by slip

Van T. Huynh, Ryan N. Smith, Ngai Ming Kwok and Jayantha Katupitiya

Abstract—Autonomous guidance of agricultural vehicles is vital as mechanized farming production becomes more prevalent. It is crucial that tractor-trailers are guided with accuracy in both lateral and longitudinal directions, whilst being affected by large disturbance forces, or slips, owing to uncertain and undulating terrain. Successful research has been concentrated on trajectory control which can provide longitudinal and lateral accuracy if the vehicle moves without sliding, and the trailer is passive. In this paper, the problem of robust trajectory tracking along straight and circular paths of a tractor-steerable trailer is addressed. By utilizing a robust combination of backstepping and nonlinear PI control, a robust, nonlinear controller is proposed. For vehicles subjected to sliding, the proposed controller makes the lateral deviations and the orientation errors of the tractor and trailer converge to a neighborhood near the origin. Simulation results are presented to illustrate that the suggested controller ensures precise trajectory tracking in the presence of slip.

I. INTRODUCTION

The agriculture industry is rapidly increasing in mechanization and autonomy. This trend is stimulated by the necessity to effectively and productively retain vast expanses of cultivated fields, with a decline in skilled workforce. Additionally, with the escalating labor cost, there is a gradually increasing difficulty in maintaining competitiveness of the farming industry. Hence, it has led to the emergence of "corporate" style farming, where large firms tend to monopolize the whole industry [1]. As a result, the agricultural industry has turned to innovation via automation.

One of the impacts of a decreased workforce and "corporatized" farming is the demand to develop autonomous agricultural tractor-trailers, which will in the coming decades play an important role in almost all systems for greenhouses and outdoor applications. Furthermore, one of the biggest difficulties in stepping towards the autonomous farming era is integrating robotic technology into farming fields. If the working environment is more undulating and uncertain, more machine intelligence is required to obtain the desired precision of operations. Autonomous tractors with such intelligence are currently under development [2]–[4], even though some of them are available commercially as "auto-steer" systems. While the precision of an agricultural task is crucially depended on how the towed implement is guided, most of those works together with studies on experimentally

Van T. Huynh and Ryan N. Smith are with the School of Systems Engineering, Queensland University of Technology, thanhvan.huynh@student.qut.edu.au ryan.smith@qut.edu.au

Ngai Ming Kwok and Jayantha Katupitiya are with the School of Mechanical and Manufacturing Engineering, University of New South Wales.

controlling towing vehicles [5], [6] concentrate on tractor guidance. However, a class of tractor-trailer modeling and control has not received much attention.

Due to the unstructured property of the ground at the farm, inevitable slip¹ exerted on the agricultural vehicles must be considered when controlling the tractor-trailer. To account for slippery effects, Pota et al. [7] proposed a dynamic model for the tractor-trailer which contained both longitudinal and side slips. Moreover, some kinematic models for the tractor alone are also depicted in Fang's work [8]–[10]. However, few studies inspect the complete tractor-trailer's kinematic model influenced by slippery effects.



Fig. 1. A tractor-trailer on farm - © Copyright Richard Croft and licensed for reuse under Creative Commons Licence

In addition, once the kinematic model containing perturbations and uncertainties is completely derived, controlling the tractor-trailer to precisely follow a prescribed trajectory is even more challenging. Besides the slippery disturbances occurring at the tractor, the trailer being towed undergoes large ground contact forces. Hence, trajectory planning and advanced control techniques developed to accurately guide the tractor-implement are non-trivial and still remain as a central part of the wider issue of building precision farming machinery. Nevertheless, most recent results are restricted to a tractor-semi trailer system, which is not steerable at the towed implement's rear axle [11]–[13].

References [11] and [12] motivate design of the controller for both the tractor and the trailer in the presence of sliding. For the tractor, besides two typical controllers for the tractor under the influence of slips have been presented

¹In the remainder of this paper, terms of "slip", "sliding", "sliding parameters" and "slippery effects" will be used interchangeably.

in [8], [9], a completely new controller will be presented based on the error dynamics recently derived in [14]. The robust backstepping technique will be utilized to synthesize a control law for the tractor. Furthermore, a Lyapunov redesign method, which was depicted by Khalil [15], will be applied in combination with the recursive tool. The usefulness of this combination is that, while the Lyapunov redesign method as well as nonlinear damping can tackle nonlinear systems with matched perturbations containing both states and inputs, the robust backstepping scheme can counteract mismatched uncertainties. For the trailer, because its dynamics contains both system uncertainties and exogenous input disturbances, there are few results that can be applied to guide it. Among the literature, methods developed in [16]–[19] are applicable to solving the problem of trailer path tracking. However, to choose a control Lyapunov function (CLF) with its derivative satisfying inequalities in Haddad’s study is non-trivial work. Likewise, there are difficulties in using Isidori’s result [17], due to the solvability of partial differential equations and forming the interconnected system before designing a controller. Furthermore, the integral-type sliding mode control proposed in Cao [18] and Castanos [19] shows potential for being applicable to the control of the trailer. Unfortunately, in those studies, the assumption that the Euclidean norm of the nonlinear coefficient matrix associated with the input is less than unity cannot be satisfied when we considered the trailer’s dynamics. During the period of searching for a suitable control design procedure for the implement, a nonlinear PI control design method has been found to be applicable. The nonlinear PI control introduced in [20] is a powerful technique to tackle nonlinear systems in the presence of perturbations and exogenous input disturbances. With the condition of bounded uncertainties and small unmeasured exogenous disturbances, the nonlinear PI controller guarantees globally uniformly boundedness of not only system states but also the unpredictable input disturbances from ambient environment.

The rest of this paper is organized as follows. In Section 2, the kinematic model being used is briefly introduced. After that, Section 3 depicts the synthesis of a control algorithm for both the tractor and steerable trailer. Then, simulation results are presented in Section 4. Finally, concluding remarks are given in Section 5.

II. KINEMATIC MODEL WITH SLIPS

The tractor-trailer to be controlled is depicted in Fig. 2. Steering wheels of the tractor-trailer are represented by single wheels along longitudinal axes of the tractor and trailer. The drive of the vehicle is via the rear wheels of the tractor. The following model description is based on that of [14]. The tractor’s off-axle length is a , and l_1 is the distance from tractor’s rear axle to tractor’s front axle. For the trailer, l_2 is the distance from trailer’s axle to the hitch point.

The tractor’s state is given by $\mathbf{q}_t = [x_t \ y_t \ \theta_t \ \delta]^T$, where (x_t, y_t) is the position of the middle point of the tractor’s rear axle in the xOy global coordinate. Similarly, the trailer’s state is given by $\mathbf{q}_i = [x_i \ y_i \ \theta_i \ \delta_i]^T$, where (x_i, y_i) is the

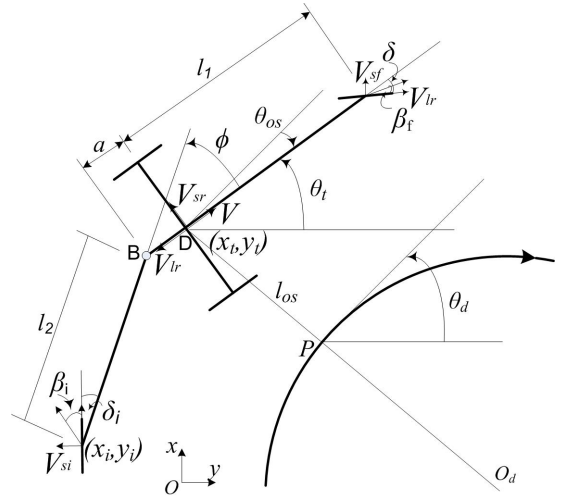


Fig. 2. The offset model for tractor with steerable trailer

position of the middle point of the trailer’s axle. Moreover, θ_t and, $\Omega_t = \dot{\theta}_t$, are the orientation and angular velocity of the tractor’s longitudinal axis. Likewise, θ_i and, $\Omega_i = \dot{\theta}_i$, are the orientation and angular velocity of the trailer’s longitudinal axis. Steering for the tractor is effected via the front wheel, with steering angle δ , while the active trailer is directed by the trailer’s steered wheel, with a steering angle δ_i . In addition, the drive speed produced by the tractor is V . Velocity V will then cause a velocity V_f at the steering wheel and a velocity V_i at the trailer’s steering wheel.

Slips are modeled by the inclusion of slip velocities in the lateral and longitudinal velocities. We use V_{lr} to represent a longitudinal slip velocity at the tractor’s rear wheels, and ($V_{lr} > 0$) if vector \mathbf{V}_{lr} is opposite to vector \mathbf{V} . V_{sr} is a side slip velocity at the tractor’s rear wheels, and ($V_{sr} > 0$) when \mathbf{V}_{sr} direction relatively points towards the left of the vehicle as described in the current figure. Also, there is a side slip V_{sf} at the front wheel of the tractor. Note that disturbance at the tractor’s steered wheel can be represented either by the slip velocity V_{sf} or by a slip angle β_f . For the disturbance acting on the towed implement, we have V_{si} or a slip angle β_i represent the side slip at the trailer’s rear axle.

Under slippery effects, the model of the tractor-trailer is given by $\mathbf{H}(t, \mathbf{q})\dot{\mathbf{q}} = \mathbf{F}(t, \mathbf{q}, \mathbf{w})$ where,

$$\mathbf{H} \in \mathbb{R}^{6 \times 6}; \mathbf{F}, \mathbf{q} \in \mathbb{R}^{6 \times 1};$$

$$\mathbf{w} = [\beta_f \ V_{lr} \ V_{sr} \ V_{si} \ 0 \ 0]^T: \text{disturbances}$$

$$\mathbf{H} = \begin{bmatrix} 1 & 0 & 0 & 0 & 0 & 0 \\ h_{21} & h_{22} & 0 & 0 & 0 & 0 \\ 0 & 0 & 1 & 0 & 0 & 0 \\ 0 & 0 & 0 & 1 & 0 & 0 \\ h_{51} & h_{52} & -1 & 0 & 1 & 0 \\ h_{61} & h_{62} & 0 & -1 & 0 & 1 \end{bmatrix}; \quad \dot{\mathbf{q}} = \begin{bmatrix} \dot{\theta}_t \\ \dot{\theta}_i \\ \dot{x}_t \\ \dot{y}_t \\ \dot{x}_i \\ \dot{y}_i \end{bmatrix}$$

$$\mathbf{F} = [f_1 \ f_2 \ f_3 \ f_4 \ 0 \ 0]^T$$

$$\begin{aligned}
h_{21} &= -a \cos(\delta_i + \phi) \sin \phi; h_{22} = l_2 \sin \phi \cos \delta_i; \\
h_{51} &= -a \sin \theta_t, h_{52} = -l_2 \sin \theta_i; \\
h_{61} &= a \cos \theta_t, h_{62} = l_2 \cos \theta_i; \\
f_1 &= \Omega_t = \frac{V - V_{lr}}{l_1} \tan(\delta + \beta_f) + \frac{V_{sr}}{l_1}; \\
f_2 &= M_1 + M_2 + M_4; \\
f_3 &= (V - V_{lr}) \cos \theta_t - V_{sr} \sin \theta_t; \\
f_4 &= (V - V_{lr}) \sin \theta_t + V_{sr} \cos \theta_t; \\
M_1 &= -(V - V_{lr}) \sin(\delta_i + \phi) \sin \phi \\
M_2 &= V_{sr} \sin(\phi) \cos(\delta_i + \phi); M_4 = -V_{si} \sin \phi.
\end{aligned}$$

For trajectory tracking, a reference path is introduced. In practice, executed paths can be reasonably approximated by a sequence of straight lines and arcs. Thus, we consider a rectilinear path and a circular path of radius R_1 . As can be seen in Fig. 2, the circle centered at O_d with radius R_1 is the reference trajectory. R_1 will approach ∞ if the predetermined path is a straight line.

To control the tractor-trailer, an error dynamics of the vehicle is used. Such error dynamics has three offset variables. The first offset variable is ϕ_{os} , which is equal to the current angle ϕ (between the tractor and trailer) less its steady state value ϕ_d (along the prescribed path). The other two offset variables are l_{os} and θ_{os} , which denote the tractor lateral offset and its orientation offset, respectively. The variables l_{os}, θ_{os} are measured with reference to the projection of point D, the middle of tractor's rear axle, onto the desired path. Particularly, $|l_{os}| = |\mathbf{DP}|$, where point P is the intersection between $O_d D$ and the prescribed path. Furthermore, we have $\theta_{os} = \theta_t - \theta_d$, with θ_d is the desired steady state value of θ_t .

According to [14], we have the offset model as follows:

$$\dot{l}_{os} = -\sigma |V - V_{lr}| \sin \theta_{os} - \sigma V_{sr} \cos \theta_{os}, \quad (1a)$$

$$\begin{aligned} \dot{\theta}_{os} &= \frac{V - V_{lr}}{l_1} \tan(\delta + \beta_f) + \frac{V_{sr}}{l_1} \\ &\quad - \sigma |V - V_{lr}| \frac{\cos \theta_{os}}{R_1 + l_{os}} + \sigma V_{sr} \frac{\sin \theta_{os}}{R_1 + l_{os}}, \end{aligned} \quad (1b)$$

$$\begin{aligned} \dot{\phi}_{os} &= \frac{1}{l_2 \cos \delta_i} \left\{ -(V - V_{lr}) \sin(\delta_i + \phi_{os} + \phi_d) \right. \\ &\quad + V_{sr} \cos(\delta_i + \phi_{os} + \phi_d) \\ &\quad - \left. \left(\frac{V - V_{lr}}{l_1} \tan(\delta + \beta_f) + \frac{V_{sr}}{l_1} \right) \times \right. \\ &\quad \left. \left(a \cos(\delta_i + \phi_{os} + \phi_d) + l_2 \cos \delta_i \right) - V_{si} \right\}, \end{aligned} \quad (1c)$$

where σ is a direction coefficient. Being referenced from the center of the prescribed circle, $\sigma = 1$ if the vehicle follows the desired path in counterclockwise direction, and $\sigma = -1$ if the vehicle follows the desired path in clockwise direction.

III. CONTROLLER DESIGN

In this section, synthesis of the nonlinear controller for the tractor-trailer will be presented. A control law for the tractor is constructed first. After that, construction of a control law for the trailer will be shown.

A. Controller Design for the Tractor

We present step by step establishment of a control input for the car-like mobile robot. Because there are two equations Eqs. (1a-1b), concerning (l_{os}, θ_{os}) offset variables, affecting control of the tractor in the model Eq. (1), the backstepping design procedure has two steps. The first step deals with Eq. (1a) to formulate a virtual control. The second step tackles Eq. (1b) and the whole tractor's model to construct a controller for the towing vehicle. However, equation (1), with lateral, orientation and hitch angle offset variables $(l_{os}, \theta_{os}, \phi_{os})$, is still primitive and cannot be directly incorporated in the design procedure. We first need to linearize the function $\tan(\delta + \beta_f)$ and change l_{os}, θ_{os} into a new coordinate. As a result of this action, the original model becomes a nominal model, augmented with additive disturbances. It is the mathematical model with additive perturbations that is directly used in the backstepping design scheme.

According to [8], there are two typical observations in actual agricultural applications. Firstly, the ground conditions, such as, gradient, friction, curvature, do not vary abruptly. Secondly, most trajectories to be followed are straight lines or circles. Hence, if the agricultural vehicles move smoothly without excessive acceleration, one may assume that the sliding parameters do not vary tremendously with time. The sliding parameters are then given by:

$$\beta_f = \bar{\beta}_f + \varepsilon_1, \quad (2)$$

where $\bar{\beta}_f$ is time-invariant, ε_1 is a time-varying variable with zero mean, and obeys a normal distribution.

Also according to [8], the steering bias β_f is normally within the range $[0, 5]$ degrees. Due to quite small values of β_f , $\tan(\delta + \beta_f)$ can be linearized as follows:

$$\tan(\delta + \beta_f) = \tan \delta + \tan \bar{\beta}_f + \varepsilon_1, \quad (3)$$

where $\varepsilon_1 = \tan \varepsilon_1 + \varepsilon$, ε is the error due to linearization approximation. From now on, for simplicity, we just write $\tan \beta_f$ instead of $\tan \bar{\beta}_f$.

Let us denote l_{os} , $\sin \theta_{os}$ and $\tan \delta$ as x_1 , x_2 and u_1 . By linearizing the $\tan(\delta + \beta_f)$, and transforming (1a-1b) in (l_{os}, θ_{os}) -coordinate to (x_1, x_2) -coordinate, we obtain a mathematical model with additive perturbations that is suitable for the recursive backstepping design scheme. Such a mathematical model is represented by the following equations:

$$\dot{x}_1 = f_1(x) + g_1(x)x_2 + F_1(x)\Delta_1(x, w), \quad (4)$$

$$\dot{x}_2 = f_2(x) + g_2(x)u_1 + F_2(x)\Delta_2(x, u, w), \quad (5)$$

where,

$$\begin{aligned}
f_1(x) &= 0; g_1(x) = -\sigma V; \\
F_1(x) &= 1; \\
f_2(x) &= -\sigma V \frac{(1-x_2^2)}{R_1+x_1}; g_2(x) = \frac{V}{l_1} \sqrt{1-x_2^2}; \\
F_2(x) &= \sqrt{1-x_2^2}; \\
\Delta_1(x, w) &= \sigma \left(V_{lr} x_2 - V_{sr} \sqrt{1-x_2^2} \right); \\
\Delta_2(x, u, w) &= \frac{V}{l_1} (\tan \beta_f + \epsilon_1) + \frac{V_{sr}}{l_1} \\
&\quad - \frac{V_{lr}}{l_1} (u_1 + \tan \beta_f + \epsilon_1) \\
&\quad + \sigma V_{lr} \frac{\sqrt{1-x_2^2}}{R_1+x_1} + \sigma V_{sr} \frac{x_2}{R_1+x_1}.
\end{aligned} \tag{6}$$

Choose a Control Lyapunov Function(CLF) as:

$$V_1 = \frac{1}{2} x_1^2, \tag{8}$$

which upon differentiating gives,

$$\dot{V}_1 = -\sigma V x_1 x_2 + x_1 \Delta_1(x, w). \tag{9}$$

Select the virtual input as,

$$\begin{aligned}
x_2 = \Phi(x_1) &= \frac{c_1}{\sigma V} x_1 + \frac{k_1}{\sigma V} x_1 \\
&= \frac{\bar{c}_1}{\sigma V} x_1 = \left(\frac{c_1 + k_1}{\sigma V} \right) x_1 = \mu x_1,
\end{aligned} \tag{10}$$

where c_1, k_1 and μ are design parameters for the controller. Thus,

$$\begin{aligned}
\dot{V}_1 &= -\sigma V x_1 \left(\frac{c_1}{\sigma V} x_1 + \frac{k_1}{\sigma V} x_1 \right) + x_1 \Delta_1(x, w) \\
&\leq -c_1 x_1^2 + \frac{\Delta_1^2(x, w)}{4k_1} \\
&\leq -W(x) + b.
\end{aligned} \tag{11}$$

$$\leq -W(x) + b. \tag{12}$$

The error state variable is:

$$z = x_2 - \Phi(x_1) = x_2 - \frac{\bar{c}_1}{\sigma V} x_1 = x_2 - \mu x_1. \tag{13}$$

So, the system can then be written as:

$$\dot{x}_1 = f_1(x) + g_1(x)(z + \Phi(x_1)) + F_1(x) \Delta_1(x, w), \tag{14}$$

$$\begin{aligned}
\dot{z} &= f_2(x) + g_2(x) u_1 + F_2(x) \Delta_2(x, u, w) \\
&\quad - \frac{\partial \Phi}{\partial x_1} (f_1(x) + g_1(x) x_2 + F_1(x) \Delta_1(x, w)).
\end{aligned} \tag{15}$$

Thus, we choose the CLF for the whole system to be,

$$V_2(x_1, x_2) = V_1(x) + \frac{1}{2} z^2. \tag{16}$$

Thus, its derivative would be,

$$\begin{aligned}
\dot{V}_2 &= \frac{\partial V_1}{\partial x_1} (f_1 + g_1 \Phi + F_1 \Delta_1) + z \left(F_2 \Delta_2 - \frac{\partial \Phi}{\partial x_1} F_1 \Delta_1 \right) \\
&\quad + z \left(f_2 + g_2 u_1 + \frac{\partial V_1}{\partial x_1} g_1 - \frac{\partial \Phi}{\partial x_1} (f_1 + g_1 x_2) \right) \\
&\leq -W(x) + b + z \left(f_2 + g_2 u_1 + \frac{\partial V_1}{\partial x_1} g_1 \right. \\
&\quad \left. - \frac{\partial \Phi}{\partial x_1} (f_1 + g_1 x_2) \right) + z \left(F_2 \Delta_2 - \frac{\partial \Phi}{\partial x_1} F_1 \Delta_1 \right).
\end{aligned} \tag{17}$$

Because $g_2(x) \neq 0$, here we take,

$$u_1 = \frac{\Psi_1(x_1, x_2) + v}{g_2}, \tag{18}$$

where v is a supplementary control, and $\Psi_1 = -a_1 z - f_2 - \frac{\partial V_1}{\partial x_1} g_1 + \frac{\partial \Phi}{\partial x_1} (f_1 + g_1 x_2)$. Hence,

$$\dot{V}_2 \leq -W(x) + b - a_1 z^2 + z \left(F_2 \Delta_2 - \frac{\partial \Phi}{\partial x_1} F_1 \Delta_1 + v \right).$$

With the designed controller u_1 as expressed in Eq. (18), the bound of the uncertainty $\Delta_2(x, u, w)$ is also affected. The remaining discussion of this subsection will be about constructing the supplementary control v based on bounds of the uncertainties Δ_1 and Δ_2 . Readers may refer to Appendix I on finding bounds of such uncertainties functions.

Let us introduce a new control parameter η , which can be selected as,

$$\eta(t, x) = \eta_0 + \frac{\rho(|x_1|) + \rho_3}{1 - \kappa_v}. \tag{19}$$

With the function η in hand, we now have enough information to apply the Lyapunov redesign technique to construct the supplementary control v . For $\varepsilon \in \mathbb{R}_+$, two cases of $\eta(t, x)|z| \geq \varepsilon$ and $\eta(t, x)|z| \leq \varepsilon$ will be considered to synthesize control laws for v .

Particularly, when $\eta(t, x)|z| \geq \varepsilon$, then choose,

$$v = -\eta(t, x) \text{sgn}(z). \tag{20}$$

Thus,

$$z \left(F_2 \Delta_2 - \frac{\partial \Phi}{\partial x_1} F_1 \Delta_1 + v \right) \leq -\eta_0 (1 - \kappa_v) |z|. \tag{21}$$

Therefore,

$$\dot{V}_2 \leq -W(x) + b - a_1 z^2 - \eta_0 (1 - \kappa_v) |z|. \tag{22}$$

When $\eta(t, x)|z| \leq \varepsilon$, then choose,

$$v = -\eta^2(t, x) \frac{z}{\varepsilon}, \tag{23}$$

Hence,

$$\dot{V}_2 \leq -W(x) + b - a_1 z^2 + z \left(-\eta^2 \frac{z}{\varepsilon} + \Delta'_2 - \Delta'_1 \right). \tag{24}$$

However, due to $\rho + \rho_3 \leq \eta(1 - \kappa_v)$, it can be easily seen that,

$$\begin{aligned} z(-\eta^2 \frac{z}{\varepsilon} + \Delta'_2 - \Delta'_1) &\leq -(1 - \kappa_v) \frac{z^2 \eta^2}{\varepsilon} + |z|(\rho + \rho_3) \\ &\leq (1 - \kappa_v) \left(-\frac{z^2 \eta^2}{\varepsilon} + |\eta||z| \right). \end{aligned} \quad (25)$$

As a result,

$$\dot{V}_2 \leq -W(x) - a_1 z^2 + \frac{(1 - \kappa_v)\varepsilon}{4} + b. \quad (26)$$

From Eqs. (22) and (26), we see that the inequality Eq. (26) is satisfied irrespective of the value of $\eta(t, x)|z|$. By choosing a_1 large and ε small enough, the state variables of x_1 and x_2 will be uniformly asymptotically bounded. In other words, since $x_1 = l_{os}$ and $x_2 = \theta_{os}$, all the offset variables will converge to a ball B_r with radius r , which depends on the design parameters in Eqs. (18), (20) and (23). In general, the controller for tractor path-following is presented in Eqs. (18), (20) and (23).

B. Controller Design for the Trailer

Notice that, once the tractor has been guided to follow a trajectory by the control law Eq. (18), the tractor's angular velocity will be equal to its desired velocity plus an error value, which is called ε'_Ω . By applying interval analysis [21] and the inclusion function of $[\varepsilon'_\Omega]$, we have,

$$\Omega_t = \frac{V - V_{lr}}{R_1} + \varepsilon'_\Omega = \frac{V}{R_1} - \frac{V_{lr}}{R_1} + \varepsilon'_\Omega = \frac{V}{R_1} + [\varepsilon_\Omega]. \quad (27)$$

Substituting Eq. (27) into Eq. (1c), we obtain the following ODE for the hitch angle offset,

$$\dot{\xi} = F(\xi) + G(\xi)u_i + \mathbf{P}(\xi)\varphi(\xi) + \mathbf{Q}(\xi)\mathbf{w}, \quad (28)$$

where $\xi = \phi_{os}$ is the hitch angle offset variable, $u_i = \tan \delta_i$ is trailer's control input and,

$$\begin{aligned} F(\xi) &= \left[-\frac{V}{l_2}q_s - \frac{V}{R_1} \frac{a}{l_2}q_c - \frac{V}{R_1} \right], \\ G(\xi) &= \left[-\frac{V}{l_2}q_c + \frac{V}{R_1} \frac{a}{l_2}q_s \right], \\ \mathbf{P}(\xi) &= [-aq_c \quad -1 \quad q_s \quad q_c], \\ \varphi^T(\xi) &= \left[\frac{[\varepsilon_\Omega]}{l_2} \quad [\varepsilon_\Omega] \quad \frac{V_{lr}}{l_2} \quad \frac{V_{sr}}{l_2} \right]^T, \\ \mathbf{Q}(\xi) &= [aq_s \quad -1 \quad q_c \quad -q_s], \\ \mathbf{w}^T &= \left[\frac{[\varepsilon_\Omega]}{l_2}u_i \quad \frac{1}{l_2} \frac{V_{si}}{\cos \delta_i} \quad \frac{V_{lr}}{l_2}u_i \quad \frac{V_{sr}}{l_2}u_i \right]^T, \\ q_s &= \sin(\phi_{os} + \phi_d), \quad q_c = \cos(\phi_{os} + \phi_d). \end{aligned}$$

Whenever the tractor successfully tracks the desired trajectory, we can proceed to provide a control for the trailer. The trailer's controller directly adjusts the hitch angle to make the hitch angle offset remain at zero. By using such approach, not only the tractor but also the trailer need to follow desired trajectories. For example, if the tractor is required to track a circular path CC_1 , and if the hitch angle are maintained at a prescribed value ϕ_d , then the trailer will also follow a

circular path which is offset from the CC_1 by a distance depending on ϕ_d . Based on the derived ODE Eq. (28), we continue to design a nonlinear PI controller for the towed implement.

First of all, if $\phi = (\phi_{os} + \phi_d) \neq \tan^{-1} \frac{R_1}{a}$ such that $G(\xi) \neq 0$, a supplementary control v can be introduced as follows,

$$u_i = \frac{v - F(\xi)}{G(\xi)}. \quad (29)$$

Therefore, Eq. (28) turns to

$$\dot{\xi} = v + \mathbf{P}(\xi)\varphi(\xi) + \mathbf{Q}(\xi)\mathbf{w}, \quad (30a)$$

$$y = \xi. \quad (30b)$$

As to synthesize a nonlinear PI control law, the supplementary control adjusting the trailer should be in the form,

$$v = \mu_1(\boldsymbol{\xi}, \boldsymbol{\omega}, y_s), \quad (31a)$$

$$\dot{\boldsymbol{\omega}} = \boldsymbol{\Omega}_1 + \mathbf{d}, \quad (31b)$$

where $\mu_1 \in \mathbb{R}$ and $\boldsymbol{\Omega}_1 \in \mathbb{R}^p$ are smooth functions, $\boldsymbol{\omega} \in \mathbb{R}^p$ is the internal state of the controller, and $y_s \in \mathbb{R}$ is the desired output. Furthermore, $\mathbf{d} \in \mathbb{R}^p$ is an additional unmeasured disturbance input so as to guarantee the robustness of the controller provided that there are small errors in the measurement of the state $\boldsymbol{\xi}$. The dimension p of the internal state $\boldsymbol{\omega}$ will be found below once a Lyapunov function for the trailer system is established.

At the first step of our design procedure, we introduce a tracking error variable $z_1 \in \mathbb{R}$, where $z_1 = y - y_s$ and $y_s = 0$ is the desired output. Consider the Lyapunov function:

$$V_1 = C_1 z_1^2 + [\varphi(y_s) - \boldsymbol{\omega}]^T \mathbf{E} [\varphi(y_s) - \boldsymbol{\omega}], \quad (32)$$

with,

$$C_1 \in \mathbb{R}_+, \quad \mathbf{E} > 0, \quad \mathbf{E} \in \mathbb{R}^{4 \times 4}, \quad \boldsymbol{\omega} \in \mathbb{R}^{4 \times 1}.$$

Taking derivative of V_1 along the solution of Eqs. (30), (32) gives,

$$\begin{aligned} \dot{V}_1 &= 2z_1 C_1 \left[\mu_1 + \mathbf{P}\boldsymbol{\omega} + \mathbf{P}[\varphi(y) - \varphi(y_s)] + \mathbf{Q}\mathbf{w} \right] \\ &\quad + 2[\varphi(y_s) - \boldsymbol{\omega}]^T \mathbf{E} [\mathbf{P}^T C_1 z_1 - \mathbf{E}\boldsymbol{\Omega}_1 - \mathbf{E}\mathbf{d}], \end{aligned} \quad (33)$$

with,

$$\mu_1 \in \mathbb{R}, \quad \boldsymbol{\Omega}_1^T = [\omega_1 \quad \omega_2 \quad \omega_3 \quad \omega_4] \in \mathbb{R}^{1 \times 4}, \quad \mathbf{d} \in \mathbb{R}^{4 \times 1}.$$

It is worth mentioning that φ in Eq. (30) contains only sliding parameters. Hence, it results in $\varphi(y) - \varphi(y_s) = 0$. By applying Young's inequality [20] and introducing a positive design parameter ε , we have bounds for the uncertain terms in Eq. (33), as follows,

$$2z_1^T C_1 \mathbf{Q}(\boldsymbol{\xi})\mathbf{w} \leq \frac{1}{\varepsilon} z_1^T C_1 \mathbf{Q}[\mathbf{Q}]^T C_1 z_1 + \varepsilon \|\mathbf{w}\|^2, \quad (34)$$

$$\begin{aligned} -2[\varphi(y_s) - \boldsymbol{\omega}]^T \mathbf{E}\mathbf{d} &\leq \frac{1}{\varepsilon} [\varphi(y_s) - \boldsymbol{\omega}]^T \mathbf{E}^2 [\varphi(y_s) - \boldsymbol{\omega}] \\ &\quad + \varepsilon \|\mathbf{d}\|^2. \end{aligned} \quad (35)$$

Based on the bounds of uncertain terms, we can now construct

$$v = \mu_1 = - \left(\frac{D_1}{C_1} + \frac{1}{2\varepsilon} \mathbf{Q} \mathbf{Q}^T C_1 \right) z_1 - \mathbf{P} \boldsymbol{\omega}, \quad (36a)$$

$$\boldsymbol{\Omega}_1 = \mathbf{E}^{-1} \mathbf{L}(\boldsymbol{\omega}, y_s) + \mathbf{E}^{-1} \mathbf{P}^T C_1 z_1, \quad (36b)$$

with $D_1 \in \mathbb{R}$ and $\mathbf{L}(\boldsymbol{\omega}, y_s) \in \mathbb{R}^{4 \times 1}$ are two design parameters. Substituting Eqs. (34-35) and (36) into the derivative \dot{V}_1 of the Lyapunov function, we obtain

$$\begin{aligned} \dot{V}_1 \leq & -2D_1 z_1^2 - 2[\boldsymbol{\varphi}(y_s) - \boldsymbol{\omega}]^T \mathbf{L}(\boldsymbol{\omega}, y_s) \\ & + \frac{1}{\varepsilon} [\boldsymbol{\varphi}(y_s) - \boldsymbol{\omega}]^T \mathbf{E}^2 [\boldsymbol{\varphi}(y_s) - \boldsymbol{\omega}] + \varepsilon \|\bar{\mathbf{w}}\|^2, \end{aligned} \quad (37)$$

where $\bar{\mathbf{w}} = [\mathbf{w}^T \mathbf{d}^T]^T$ stand for the combined exogenous disturbance input. Due to the tube shape of the set-valued map Φ , we can establish $\mathbf{L}(\boldsymbol{\omega}, y_s)$ as follows,

$$\mathbf{L}^T(\boldsymbol{\omega}, y_s) = [L_1 \quad L_2 \quad L_3 \quad L_4], \quad (38)$$

$$L_i(\boldsymbol{\omega}, y_s) = -\alpha_i \left(\omega_i - \text{sgn}(\omega_i) |\Psi_i| \right), \quad (39)$$

with $i = 1, 2, 3, 4$ and $\alpha_i > 0$ are design parameters. The establishment of \mathbf{L} satisfying Eqs. (38-39) makes the term $\boldsymbol{\omega}^T \mathbf{L}(\boldsymbol{\omega}, y_s)$ in Eq. (37) negative. As a result, by choosing suitable ε , \mathbf{E} and \mathbf{L} , the tracking error would converge to a ball $\mathbf{B}(0, r_t)$, which is centered at 0 and has radius r_t depending on $(\varepsilon, \mathbf{E}, \mathbf{L}, \bar{\mathbf{w}})$.

IV. RESULTS

Results of applying the controllers constructed in previous sections to the tractor-trailer are presented in this section. For tractor-trailer path-following, effectiveness of the tractor's controller (represented by Eqs. (18), (20) and (23)) and the steerable trailer's controller (represented by Eqs. (29), (36), (38) and (39)) is simulated.

The reference propulsion is equal to $V = 3 \text{ m/s} = 10.8 \text{ km/h}$. Due to the fact that the implement carrying out the agricultural task is subjected to ground contact forces, the sliding occurring at the trailer's rear axle is larger than slip at the tractor's rear axle and elsewhere. Hence, the sliding parameters used in the simulation are selected as $V_{sf} = 0.04 \text{ m/s}$, $V_{sr} = 0.04 \text{ m/s}$, $V_{lr} = 0.02 \text{ m/s}$, $V_{si} = 0.08 \text{ m/s}$. Design parameters for the tractor's controller are chosen as $c_1 = 0.6$, $k_1 = 0.6$, $a_1 = 0.01$, $a_2 = 1.05$, $\eta_0 = 1$. The parameter ε deciding when to switch on the control law Eq. (23) is equal to 0.1. Furthermore, design parameters for the trailer's controller are selected as $C_1 = 10$, $\mathbf{E} = 0.001 \mathbf{I}$, $N_1 = 0$, $D_1 = 10$ and $\alpha_i = 20$ for all $i = 1, 2, 3, 4$.

We will consider controlling the vehicle to track a circular path and a straight line trajectory in the following subsections. For all of the cases, the tractor's controller becomes effective to regulate the towing vehicle at the beginning. About two seconds later, the trailer's controller is activated to guide the towed implement. Moreover, the tractor-trailer is originally located at $[x_t \quad y_t \quad x_i \quad y_i]^T = [0 \quad 3 \quad 0 \quad 0]^T$.

A. Following a circular path

The prescribed path is a circle of radius $R_1 = 5 \text{ m}$. The desired hitch angle is $\phi_d = 14.4^\circ \approx 0.251 \text{ rad}$. In Fig. 3, the prescribed circle is in red, the tractor trajectory is in blue, and the trailer trajectory is in green. Figure 3 shows that both the tractor and the trailer follow the circular paths after five seconds. We can see a sudden, tolerable change in the trajectory of the trailer near $(2.1, 5.5)$ of the (x, y) -coordinate. This sudden change happens when the trailer's controller is switched on at 2 s. After 2 s, the trailer also follows a circular path which is offset from the 5 m prescribed circle. This is due to the fact that the hitch angle of the tractor-trailer is kept at ϕ_d while the tractor has been guided to follow the 5 m circle. The offset variables after

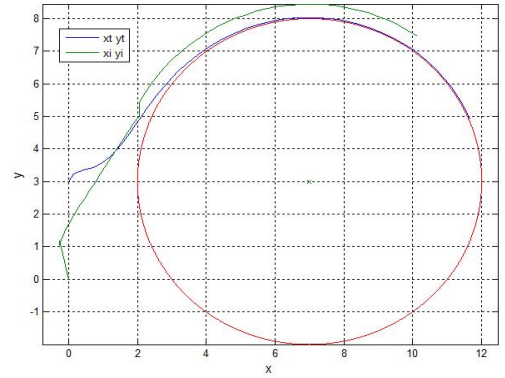


Fig. 3. The agricultural vehicle tracks a circular path

5 s are plotted in Fig. 4. All of the lateral, orientation and hitch angle offsets converge to near zero. On the other hand, the system variables are confined to a ball B_r at its steady state as what we confirmed in Sections 3. Particularly, the lateral offset, when $t \rightarrow \infty$, is less than 0.07 m. This offset is acceptably small when considering the large scale of the field.

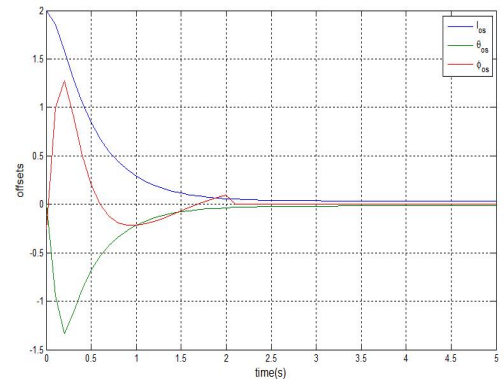


Fig. 4. Offset variables for the 5-second simulation

B. Following a straight line

As $R_1 \rightarrow \infty$, the reference curve can be seen as a straight line. Thus, in order to make the agricultural vehicle track a straight line, we assign the radius of the reference curve to a

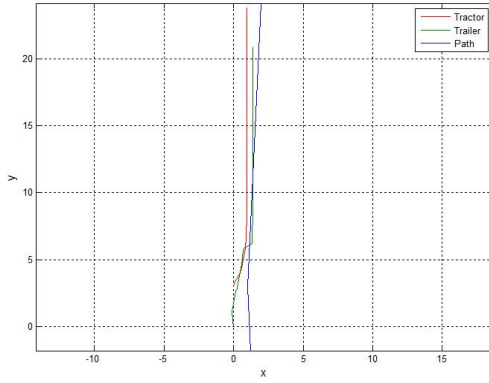


Fig. 5. Tracking a straight line

large value. If we select $R_1 = 100000$ m, the reference path will almost become a straight line, which is represented by the blue curve in Fig 5. Additionally, the tractor's trajectory is in red and the trailer's trajectory is in green. All of the design parameters are the same as those used to make the agricultural vehicle track a circular path. In case that the desired hitch angle is zero, then the trajectories of the tractor and trailer are nearly matched. Otherwise, if we choose $\phi_d = 0.251$ rad, the trajectory of the trailer is a straight line which is parallel to the trajectory of the tractor. These trajectories are plotted in Fig. 5.

C. Following a rectilinear-arc trajectory

Figure 6 illustrates how the tractor-trailer follows combined paths. The vehicle is guided to go along a straight line, an arc, and then a straight line consecutively. Similar to simulation results above, we denote the tractor's trajectory in red and the trailer's trajectory in green. In this case, distance between trajectories of the tractor and trailer is maintained at 0.45 m.

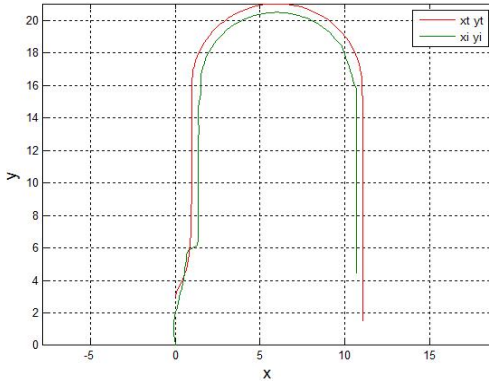


Fig. 6. Tracking a straight-arc line

Apart from small ranges of trajectories around rectilinear-arc connecting points, both the tractor and trailer can successfully follow the combined paths. Around the connecting points, there is slight variation in the trailer's paths. This phenomenon occurs because the desired hitch angle ϕ_d need to be varied when the vehicle makes a turn. More specifically,

the set-point ϕ_d when the vehicle following a straight line is different from that when the vehicle goes along a circle. Thus, such slight variation in the trailer's paths shows that the desired hitch angle is gradually changing from one value to another value.

V. CONCLUSIONS AND FUTURE WORKS

We have proposed a solution for the trailer path-tracking issue as a result of applying nonlinear PI control technique. The nonlinear PI controller dynamics consisting of integral actions have assured the asymptotic tracking of constant set-points. One of the consequences of such a controller is that the closed-loop system is robust against uncertain parameters, as well as exogenous disturbance inputs. Another consequence is that the implement could track either a circular path or a straight line. To this point, too little attention has been paid to steerable implement influenced by skid. Moreover, research to date has tended to focus on tractor-semi trailer rather than tractor-steerable trailer. Several studies have produced resolutions to the tractor-active trailer's path-tracking issue, but there is still insufficient work for such problem with the existence of slips. Therefore, the answer in this research functioned as a more general solution to the current issue of towed implement's guidance, regardless whether the trailer was active or passive.

VI. ACKNOWLEDGEMENT

Some parts of this paper are excerpted from the corresponding author's thesis at the University of New South Wales.

APPENDIX I

The relevant function bounds utilized in Subsection III-A is now listed. We proceed to find the bounds for the complicated function Δ_2 and, then, the simpler one Δ_1 . Firstly, we have,

$$\Psi_1(x_1, x_2) \leq |a_1\mu + \sigma V||x_1| + |a_1 + \sigma\mu V||x_2| + |\sigma V| \frac{|1 - x_2^2|}{|R_1 + x_1|}. \quad (40)$$

Because $R_1^2 > l_2^2 - a^2$, we can assume further that whenever the tractor is inside the prescribed circle, $x_1 < 0$, then x_1 also satisfies the condition $|x_1| = |l_{os}| \leq \frac{R_1}{a_2}$ with $(a_2 > 1)$. Hence, it leads to,

$$\Psi_1(x_1, x_2) \leq k_2|x_1| + k_3, \quad (41)$$

where,

$$k_2 = |a_1\mu + \sigma V|; k_3 = |a_1 + \sigma\mu V| + \frac{|\sigma V|a_2}{(a_2 - 1)R_1}. \quad (42)$$

Thus, it can be inferred that,

$$\begin{aligned}\Delta'_2(x, u, w) &= F_2(x)\Delta_2(x, u, w) \\ &\leq \frac{|V - V_{lr}|}{l_1}(|\tan \beta_f| + |\epsilon_1|) + \frac{|V_{sr}|}{l_1} \\ &\quad + \frac{|\sigma|a_2}{(a_2 - 1)R_1}(|V_{lr}| + |V_{sr}|) \\ &\quad + \frac{|V_{lr}|}{|V|}(k_2|x_1| + k_3 + v) \\ &\leq \rho(|x_1|) + \kappa_v|v|,\end{aligned}\quad (43)$$

where,

$$\rho(|x_1|) = \rho_1(|x_1|) + \rho_2, \quad (44)$$

$$\rho_1(|x_1|) = \left(k_2 \frac{|V_{lr}|}{|V|}\right)|x_1|, \quad (45)$$

$$\begin{aligned}\rho_2 &= \frac{|V - V_{lr}|(|\tan \beta_f| + |\epsilon_1|) + |V_{sr}|}{l_1} \\ &\quad + \frac{|\sigma|a_2(|V_{lr}| + |V_{sr}|)}{(a_2 - 1)R_1} + k_3 \frac{|V_{lr}|}{|V|},\end{aligned}\quad (46)$$

$$\kappa_v = \frac{|V_{lr}|}{|V|}. \quad (47)$$

The bound of the uncertainty Δ_1 would be

$$\begin{aligned}-\frac{\partial \Phi}{\partial x_1} F_1 \Delta_1 &\leq \left| \frac{\partial \Phi}{\partial x_1} \right| \|F_1\| |\Delta_1| \\ &\leq \frac{\bar{c}_1}{|V|} (|V_{lr}| + |V_{sr}|) = \rho_3.\end{aligned}\quad (48)$$

APPENDIX II

According to [14], we will have, in the sense of 3σ of normal distribution parameters, $V_{lr} \in [\underline{V}_{lr}, \bar{V}_{lr}]$, $V_{sr} \in [\underline{V}_{sr}, \bar{V}_{sr}]$, where $\bar{\bullet}$ and $\underline{\bullet}$ represents the upper bound and lower bound of a parameter respectively. Along with bounded $[\epsilon_\Omega]$, it can be easily seen that φ in Eq. (30) belongs to $\Phi(y)$, which then has the shape of a tube. The lower bound and upper bound of $\Phi(y)$ are,

$$\underline{\Phi}^T(y) = \left[\frac{\underline{\epsilon}_\Omega}{l_2} \quad \underline{\epsilon}_\Omega \quad \frac{V_{lr}}{l_2} \quad \frac{V_{sr}}{l_2} \right]^T, \quad (49a)$$

$$\bar{\Phi}^T(y) = \left[\frac{\bar{\epsilon}_\Omega}{l_2} \quad \bar{\epsilon}_\Omega \quad \frac{\bar{V}_{lr}}{l_2} \quad \frac{\bar{V}_{sr}}{l_2} \right]^T. \quad (49b)$$

For easier design of the controller in the remaining discussion of this part, we can construct Φ which has the lower and upper bounds symmetric with respect to zero, i.e.

$$\underline{\Phi}^T(y) = [-\Psi_1 \quad -\Psi_2 \quad -\Psi_3 \quad -\Psi_4]^T, \quad (50a)$$

$$\bar{\Phi}^T(y) = [\Psi_1 \quad \Psi_2 \quad \Psi_3 \quad \Psi_4]^T, \quad (50b)$$

where elements Ψ_i are positive, and,

$$\Psi_1 = \max \left\{ \left| \frac{\underline{\epsilon}_\Omega}{l_2} \right|, \left| \frac{\bar{\epsilon}_\Omega}{l_2} \right| \right\}; \Psi_2 = \max \{ |\underline{\epsilon}_\Omega|, |\bar{\epsilon}_\Omega| \},$$

$$\Psi_3 = \max \left\{ \left| \frac{V_{lr}}{l_2} \right|, \left| \frac{\bar{V}_{lr}}{l_2} \right| \right\}; \Psi_4 = \max \left\{ \left| \frac{V_{sr}}{l_2} \right|, \left| \frac{\bar{V}_{sr}}{l_2} \right| \right\}.$$

REFERENCES

- [1] R. Eaton, J. Katupitiya, K. W. Siew, and K. S. Dang, "Precision guidance of agricultural tractors for autonomous farming," in *Proceedings of 2008 IEEE International Systems Conference, SysCon 2008*, Montreal, QC, Canada, 2008, pp. 314–321.
- [2] B. Thuilot, C. Cariou, P. Martinet, and M. Berducot, "Automatic guidance of a farm tractor relying on a single cp-dgps," *Auton. Robots*, vol. 13, no. 1, pp. 53–71, 2002.
- [3] J. F. Reid, "Precision guidance of agricultural vehicles," The University of Illinois at Urbana-Champaign, Tech. Rep., 1998.
- [4] T. S. Stombaugh, E. R. Benson, and J. W. Hummel, "Guidance control of agricultural vehicles at high field speeds," *Transactions of the American Society of Agricultural Engineers*, vol. 42, no. 2, pp. 537–544, 1999.
- [5] T. Ryo, N. Noboru, and M. Akira, "Automatic guidance with a laser scanner for a robot tractor in an orchard," in *Proceedings of the International Conference on Automation Technology for Off-road Equipment, ATOE 2004*, Kyoto, Japan, 2004, pp. 369–373.
- [6] T. Bell, "Automatic tractor guidance using carrier-phase differential gps," *Computers and Electronics in Agriculture*, vol. 25, no. 1-2, pp. 53–66, 2000.
- [7] H. Pota, J. Katupitiya, and R. Eaton, "Simulation of a tractor- implement model under the influence of lateral disturbances," in *Proceedings of the 46th IEEE Conference on Decision and Control*, New Orleans, LA, United States, 2007, pp. 596–601.
- [8] H. Fang, R. Fan, B. Thuilot, and P. Martinet, "Trajectory tracking control of farm vehicles in presence of sliding," *Robotics and Autonomous Systems*, vol. 31, pp. 828–839, 2006.
- [9] R. Eaton, J. Katupitiya, H. Pota, and K. W. Siew, "Trajectory tracking control of farm vehicles in presence of sliding," in *Proceedings of International Conference on Advanced Intelligent Mechatronics*, Singapore, 2009, pp. 1873–1878.
- [10] R. Lenain, B. Thuilot, C. Cariou, and P. Martinet, "Adaptive control for car like vehicles guidance relying on rtk gps: Rejection of sliding effects in agricultural applications," in *Proceedings of IEEE International Conference on Robotics and Automation*, vol. 1, Taipei, Taiwan, 2003, pp. 115–120.
- [11] J.-Y. Wang and M. Tomizuka, "Gain-scheduled h-inf loop-shaping controller for automated guidance of tractor-semitrailer combination vehicles," in *the American Control Conference*, 2000, pp. 2033–2037.
- [12] P. Hingwe, A. K. Packard, and M. Tomizuka, "Linear parameter varying controller for automated lane guidance-experimental study on tractor semi-trailers," *IEEE Transactions on Control Systems*, vol. 10, pp. 793–806, Nov. 2002.
- [13] Z. Leng and M. A. Minor, "A simple tractor-trailer backing control law for path following with side-slope compensation," in *Proc. IEEE Int Robotics and Automation (ICRA) Conf*, 2011, pp. 2386–2391.
- [14] V. T. Huynh, J. Katupitiya, N. M. Kwok, and R. P. Eaton, "Derivation of an error model for tractor-trailer path-tracking," in *International Conference on Intelligent Systems and Knowledge Engineering (ISKE)*, Hangzhou, China, 2010, pp. 60–67.
- [15] H. K. Khalil, *Nonlinear Systems, 3rd Edition*. Prentice Hall, Upper Saddle River, New Jersey, 2002.
- [16] Fausz, J. L., Chellaboina, V. Sekhar, Haddad, and W. M., "Inverse optimal adaptive control for non-linear uncertain systems with exogenous disturbances," *International Journal of Adaptive Control and Signal Processing*, vol. 14, no. 1, pp. 1–38, 2000.
- [17] A. Isidori and T. J. Tarn, "Robust regulation for nonlinear systems with gain-bounded uncertainties," *IEEE Transactions on Automatic Control*, vol. 40, no. 10, pp. 1744–1754, 1995.
- [18] W.-J. Cao and J.-X. Xu, "Nonlinear integral-type sliding surface for both matched and unmatched uncertain systems," *IEEE Transactions on Automatic Control*, vol. 49, no. 8, pp. 1355–1360, 2004.
- [19] F. Castanos and L. Fridman, "Analysis and design of integral sliding manifolds for systems with unmatched perturbations," *IEEE Transactions on Automatic Control*, vol. 51, no. 5, pp. 853–858, 2006.
- [20] P. V. K. Randy A. Freeman, *Robust Nonlinear Control Design: State-Space and Lyapunov Techniques*. Birkhauser Boston, 1996.
- [21] O. D. Luc Jaulin, Michel Kieffer and E. Walter, *Applied Interval Analysis*. Springer-Verlag London, 2001.